

# A complete 3D numerical study of the effects of pseudoscalar-photon mixing on quasar polarizations

Nishant Agarwal<sup>1</sup>, Pavan K. Aluri<sup>2</sup>, Pankaj Jain<sup>2</sup>, Udit Khanna<sup>2\*</sup>, and Prabhakar Tiwari<sup>2</sup>

<sup>1</sup>*McWilliams Center for Cosmology,  
Department of Physics, Carnegie Mellon University,  
Pittsburgh, PA - 15213, USA*

<sup>2</sup>*Department of Physics,  
Indian Institute of Technology, Kanpur - 208016, India*

We present the results of three-dimensional simulations of quasar polarizations in the presence of pseudoscalar-photon mixing in the intergalactic medium. The intergalactic magnetic field is assumed to be uncorrelated in wave vector space but correlated in real space. Such a field may be obtained if its origin is primordial. Furthermore we assume that the quasars, located at cosmological distances, have negligible initial polarization. In the presence of pseudoscalar-photon mixing we show, through a direct comparison with observations, that this may explain the observed large scale alignments in quasar polarizations within the framework of big bang cosmology. We find that the simulation results give a reasonably good fit to the observed data.

## I. INTRODUCTION

In a recent paper [1] it was shown that pseudoscalar-photon mixing in the presence of correlated intergalactic magnetic fields might provide an explanation for the observed large scale alignment of quasar polarizations at visible wavelengths [2–4]. The alignment is seen over cosmologically large distances of order Gpc [2–8]. In [4], the authors argue that it is very unlikely that the effect originates due to interstellar extinction. The effect is puzzling within the framework of big bang cosmology since we do not expect astrophysical objects to be correlated over such large distances. There is also direct evidence that other properties of these objects, such as, polarization position angles at radio frequencies or position angles of parsec-scale jets, do not show any large scale alignment [9]. Hence the effect does not seem to be intrinsic to these sources and might arise due to propagation. Furthermore the propagation effect must not affect radio polarizations since these do not show any alignment. Pseudoscalar-photon mixing is a good candidate to explain the alignment of quasar optical polarizations since it is negligible at radio frequencies. Large scale correlations in the intergalactic magnetic field could lead to such an alignment over large distances [1].

In [1], it was assumed that the intergalactic magnetic field may be obtained by a simple cosmological evolution of the primordial magnetic field [10–14] within the framework of big bang cosmology. It was assumed that visible radiation from distant quasars is unpolarized at the source. It acquires polarization due to its mixing with hypothetical low mass pseudoscalars in background magnetic fields [15–26]. Such pseudoscalars arise in many extensions of the standard model of particle physics [27–35]. It was shown that the linear polarization angle of electromagnetic radiation from quasars separated over large distances becomes aligned due to correlations in the background magnetic field [1]. In [1] the authors restricted their attention to quasars that are aligned in one dimension, along the line of sight. In the current paper we present the results of a general three-dimensional numerical analysis of this problem, and show by a direct comparison with observations that such an effect can explain the observed large scale alignments in quasar polarizations.

The mixing of photons with pseudoscalars has many interesting astrophysical and cosmological implications [5, 36–53]. It affects both the intensity and polarization of radiation. Furthermore it also changes its spectral characteristics [54–58]. Extensive laboratory and astrophysical searches of these particles have led to stringent limits on their masses and couplings [38, 47, 59–79]. Some astrophysical observations also appear to indicate a positive signature of pseudoscalar-photon mixing [53, 80].

The intergalactic magnetic field is not known very well. In most treatments of pseudoscalar-photon mixing through intergalactic space it is assumed that the background medium may be split into a large number of uncorrelated domains. The domain size is typically taken to be of order Mpc with the magnetic field in each domain of order nG [43, 44, 46]. The magnetic field in different domains points in random directions and is uncorrelated. Here we assume that the background magnetic field is of primordial origin [10–14]. We also consider discretized real space consisting of a large number of cells or domains of equal size. Each domain is assumed to be cubical of side  $r_G$ . The

---

\* Present address: Harish-Chandra Research Institute, Allahabad - 211019, India

$j^{\text{th}}$  component of the magnetic field,  $B_j(\mathbf{r})$ , in real space is given by the discrete Fourier transform,

$$B_j(\mathbf{r}) = \frac{1}{V} \sum \mathbf{b}_j(\mathbf{k}) e^{i\mathbf{k} \cdot \mathbf{r}}, \quad (1)$$

where  $V$  is the volume in real space and  $\mathbf{b}_j(\mathbf{k})$  is the  $j^{\text{th}}$  component of the magnetic field in wave vector space. The magnetic field is assumed to be uniform in each domain. We may write the two point correlations of  $\mathbf{b}_j(\mathbf{k})$  as,

$$\begin{aligned} \langle \mathbf{b}_i(\mathbf{k}) \mathbf{b}_j^*(\mathbf{q}) \rangle &= \delta_{\mathbf{k},\mathbf{q}} P_{ij}(\mathbf{k}) M(k) \\ &= \delta_{\mathbf{k},\mathbf{q}} \sigma_{ij}^2(\mathbf{k}), \end{aligned} \quad (2)$$

where  $\sigma_{ij}^2(\mathbf{k}) = P_{ij}(\mathbf{k}) M(k)$ ,  $k = |\mathbf{k}|$  and  $P_{ij}(\mathbf{k}) = \left( \delta_{ij} - \frac{k_i k_j}{k^2} \right)$  is the projection operator. The function  $M(k)$  shows a power law behaviour,

$$M(k) = A k^{n_B}, \quad (3)$$

where  $n_B$  is the power spectral index. The power law dependence of this correlation function would lead to correlations in the magnetic field in real space over large distances. This is in contrast to the assumption made in most treatments of pseudoscalar-photon mixing through intergalactic space [43, 44, 46]. The constant  $A$  in Eq. 3 is fixed by demanding that

$$\sum_i \langle B_i(\mathbf{r}) B_i(\mathbf{r}) \rangle = B_0^2, \quad (4)$$

where we assume the value of about 1 nG [12, 81, 82] for  $B_0$ .

The value of the spectral index  $n_B$  has been obtained by making a best fit to the matter and CMB power spectrum [81]. This fit gives,  $n_B = -2.37$ . A fully scale invariant power spectrum would correspond to the value  $n_B = -3$ . We expect that the intergalactic medium may be turbulent on short distance scales. In this case we may expect the magnetic field to obey a Kolmogorov power spectrum for distance scales much smaller than the size of the system. A similar model is also applicable to the galactic medium, where both the plasma density and the magnetic field are known to show a Kolmogorov power spectrum [83, 84]. Hence it might be more appropriate to assume that  $n_B$  has some dependence on  $k$ . Here we shall simply treat  $n_B$  as a fixed parameter, independent of  $k$ . The spectrum may also have a low  $k$  cutoff,  $k_{\min}$ , which will imply a cutoff on correlations in real space for distances larger than  $r_{\max} = k_{\min}^{-1}$ . Here we shall assume that  $r_{\max}$  is larger than the size of our system, which we take to be of the order of a few Gpc. Hence we may simply set it equal to infinity. The large scale correlations induced among quasar polarizations crucially depend on this parameter. If this parameter is much smaller than 1 Gpc, then the mechanism proposed in [1] may not work. Alternatively we may argue that the observation of large scale correlations in quasar polarizations might be an indication that  $r_{\max} \geq 1$  Gpc. We emphasize that a magnetic field with such large distance correlations may be generated within the framework of the big bang model. The perturbations generated at the time of inflation have wavelengths extending up to the horizon in the current era. The Cosmic Microwave Background (CMB) anisotropies show significant power in the quadrupole, which implies correlations over the entire sky. The matter spectrum, however, gets significantly modified due to evolution after decoupling and correlations at such large distances get suppressed. However, the magnetic field need not evolve in the same manner as the non-relativistic matter.

In our analysis we first ignore cosmological evolution and assume a flat space-time. We are interested in radiation from quasars located at redshifts of order unity. In this case our neglect of cosmological evolution would lead to an error of order unity, which is comparable to other errors, such as in the modelling of the intergalactic magnetic field. So far most of the literature on pseudoscalar-photon mixing in a background magnetic field has ignored cosmological evolution. We next also take cosmological evolution into account.

A useful statistic to test for alignment of quasar polarizations is defined as follows [2, 6]. We first define a measure of dispersion,  $d_k$ , in the neighbourhood of the  $k^{\text{th}}$  quasar,

$$d_k = \frac{1}{n_v} \sum_{i=1}^{n_v} \cos[2(\psi_i + \Delta_{i \rightarrow k}) - 2\psi_k]. \quad (5)$$

Here  $\psi_i$  are the polarization angles of the nearest neighbours of the quasar at position  $k$ . We include a total of  $n_v$  nearest neighbours. The nearest neighbours also include the polarization angle of the  $k^{\text{th}}$  quasar. The concept of nearest neighbours requires a measure of distance. In a curved space we do not have a unique definition of distance. Here we use comoving distance as well as angular diameter distance for this purpose. When we include cosmological

evolution, we avoid this problem by locating our simulated sources at the precise positions of the observed sources. The polarizations at two different angular positions are compared by making a parallel transport from their location to the position of the  $k^{\text{th}}$  quasar along the great circle joining these points on the celestial sphere. This induces the factor  $\Delta_{i \rightarrow k}$ , included in the definition of  $d_k$ . The parallel transport is required since we are comparing polarizations located at different points on the surface of the celestial sphere. If this parallel transport factor is not included then the resulting statistic is not invariant under coordinate transformations [6]. We next maximize  $d_k$  as a function of  $\psi_k$ . The resulting value of  $\psi_k$  is interpreted as the mean polarization angle at the position  $k$  and the corresponding maxima of the function in Eq. 5 gives an estimate of  $d_k$ . The statistic may now be defined as [2, 6],

$$S_D = \frac{1}{n_s} \sum_{k=1}^{n_s} d_k|_{\text{max}}, \quad (6)$$

where  $n_s$  is the total number of sources in the data. A large value of  $S_D$  indicates a strong alignment between polarization vectors. In our analysis we shall compute this statistic theoretically and compare the corresponding values obtained by observations [2–4, 6] in order get an estimate of the model parameters.

A potential problem with our hypothesis that the alignment is caused by pseudoscalar-photon mixing is discussed in Ref. [85]. It is observed that in most cases these quasars show negligible circular polarization [4, 86]. So far this has been seen only in a small sample. Pseudoscalar-photon mixing predicts a larger circular polarization and hence may not consistently explain the data. The authors argue that if we assume the incident light to be natural white light, then due to decoherence the circular polarization is predicted to be zero, consistent with observations. However, circular polarization is observationally found to be very small even with a broadband filter. In this case theory does indicate a significant circular polarization which is not in agreement with the data. Here we address this issue partially. We point out that there exist many other effects which may cause decoherence and hence reduce the predicted circular polarization. For example, in most treatments the medium is assumed to be uniform. Alternatively one assumes a large number of domains with different properties but each individual domain is assumed to be uniform. In reality the medium, at any reasonable length scale, shows fluctuations both in space and time. Since the background magnetic field is not uniform, the pseudoscalar particle produced would not have the same energy and momentum as that of the incident photon. This acts as another source of decoherence and will suppress the circular polarization. We show this explicitly by considering a model space varying magnetic field. We find that if the magnetic field shows rapid variations in space, then the circular polarization is greatly reduced in comparison to the linear polarization. Furthermore we argue that a time varying medium may also lead to suppression of circular polarization.

## II. PSEUDOSCALAR-PHOTON MIXING IN AN EXPANDING UNIVERSE

In this section we give the basic equations of pseudoscalar-photon mixing in an expanding universe [87–89]. We assume the standard Friedmann-Robertson-Walker (FRW) metric, with the curvature parameter  $k = 0$ , using conformal time. The metric may be written as,

$$g_{\mu\nu} = \begin{pmatrix} a^2 & 0 & 0 & 0 \\ 0 & -a^2 & 0 & 0 \\ 0 & 0 & -a^2 & 0 \\ 0 & 0 & 0 & -a^2 \end{pmatrix} = a^2 \eta_{\mu\nu}, \quad (7)$$

where  $a$  is the scale parameter and  $\eta_{\mu\nu}$  the Minkowski metric.

### A. Mixing with pseudoscalars

The action of the electromagnetic field  $F_{\mu\nu}$  coupled to a pseudoscalar field  $\phi$  may be written as,

$$S = \int d^4x \sqrt{-g} \left[ -\frac{1}{4} F_{\mu\nu} F^{\mu\nu} - \frac{1}{4} g_\phi \phi F_{\mu\nu} \tilde{F}^{\mu\nu} + \frac{1}{2} (\omega_p^2 a^{-3}) A_\mu A^\mu + \frac{1}{2} g^{\mu\nu} \phi_{,\mu} \phi_{,\nu} - \frac{1}{2} m_\phi^2 \phi^2 \right]. \quad (8)$$

Here  $g_\phi$  is the coupling of  $\phi$  with the electromagnetic field. We have also written an effective photon mass term. This corresponds to the effective mass  $\omega_p^2 a^{-3}$  it acquires due to the medium, where  $\omega_p$  is the plasma frequency. In Eq. 8

we have ignored any self couplings of the scalar field. The equation of motion for the scalar field may be written as,

$$-\frac{\partial^2 \chi}{\partial \eta^2} + \nabla^2 \chi = -\frac{g_\phi}{a}(a^2 \mathbf{E}) \cdot (a^2 \mathbf{B}) + m_\phi^2 a^2 \chi, \quad (9)$$

where we have replaced  $\phi$  by  $\frac{\chi}{a}$ . In Eq. 9,  $\mathcal{B}_i + B_i = \frac{1}{2}\epsilon_{ijk}a^2 F^{jk}$  is the magnetic field,  $E_i = a^2 F^{0i}$  the usual electric field,  $\mathcal{B}$  the background magnetic field, and  $\mathbf{B}$  the magnetic field of the wave. The Maxwell's equations in curved space-time may be written as,

$$\nabla \cdot (a^2 \mathbf{E}) = -\frac{g_\phi}{a} \nabla \chi \cdot (a^2 \mathbf{B}) + \left( \frac{\omega_p^2}{a} \right) A_0, \quad (10)$$

$$\nabla \times (a^2 \mathbf{E}) + \frac{\partial(a^2 \mathbf{B})}{\partial \eta} = 0, \quad (11)$$

with

$$\frac{\partial(a^2 \mathcal{B})}{\partial \eta} = 0, \quad (12)$$

$$\nabla \times (a^2 \mathbf{B}) - \frac{\partial(a^2 \mathbf{E})}{\partial \eta} = \frac{g_\phi}{a} (\nabla \chi \times a^2 \mathbf{E}) + \frac{g_\phi}{a} (a^2 \mathcal{B}) \frac{\partial \chi}{\partial \eta} + \left( \frac{\omega_p^2}{a} \right) \mathbf{A}, \quad (13)$$

$$\nabla \cdot (a^2 \mathbf{B}) = 0, \quad (14)$$

where  $\mathbf{A}$  represents the vector potential. In the above equations we have assumed a uniform background magnetic field and approximated  $\mathcal{B} + \mathbf{B} \approx \mathcal{B}$  as  $|\mathcal{B}| \gg |\mathbf{B}|$ . Here we also ignore the term containing derivatives of the scale factor,  $a$ , since the time scale for cosmological evolution is much larger in comparison to other times scales in the problem. Now we take the curl of Faraday's Law, and use the above equations to get the wave equation for  $\mathbf{E}$ ,

$$-\frac{\partial^2(a^2 \mathbf{E})}{\partial \eta^2} + \nabla^2(a^2 \mathbf{E}) = \frac{\omega_p^2}{a}(a^2 \mathbf{E}) + \frac{g_\phi}{a}(a^2 \mathcal{B}) \frac{\partial^2 \chi}{\partial \eta^2}. \quad (15)$$

The time dependence of the resulting solution may be expressed as,

$$(a^2 \mathbf{E}) \propto \exp(-i\omega\eta) = \exp\left[-i\omega \int \frac{dt}{a(t)}\right]. \quad (16)$$

We also note that  $\omega(t)a(t) = \omega_0$ , where  $\omega_0$  is the frequency at the current time.

## B. Mixing solution

We choose the comoving coordinate system with the  $z$ -axis as the direction of propagation. In a particular domain the magnetic field is assumed to be uniform. Only the component of  $\mathbf{E}$  parallel to the background magnetic field mixes with  $\chi$ . We also define  $\mathcal{A} = \frac{(a^2 \mathbf{E})}{\omega}$  and replace  $(a^2 \mathbf{E})$  by  $\omega \mathcal{A}$ . We write the field equations of  $\mathcal{A}_\parallel$  and  $\chi$  as,

$$(\omega^2 + \partial_z^2) \begin{pmatrix} \mathcal{A}_\parallel \\ \chi \end{pmatrix} - M \begin{pmatrix} \mathcal{A}_\parallel \\ \chi \end{pmatrix} = 0, \quad (17)$$

where,

$$M = \begin{pmatrix} \frac{\omega_p^2}{a} & -\frac{g_\phi}{a}(a^2 \mathcal{B}_\perp)\omega \\ -\frac{g_\phi}{a}(a^2 \mathcal{B}_\perp)\omega & \frac{\omega_p^2}{m_\phi^2 a^2} \end{pmatrix}. \quad (18)$$

Here,  $\mathcal{B}_\perp$  is the transverse component of  $\mathcal{B}$  and  $\omega$  is the frequency of radiation at the propagation domain. Due to expansion the observed energy today is redshifted. Hence we replace  $\omega \rightarrow \frac{\omega}{a}$ . Finally the mixing matrix may be written as,

$$M = \begin{pmatrix} \frac{\omega_p^2}{a} & -\frac{g_\phi}{a^2}(a^2\mathcal{B}_\perp)\omega \\ -\frac{g_\phi}{a^2}(a^2\mathcal{B}_\perp)\omega & m_\phi^2 a^2 \end{pmatrix}. \quad (19)$$

We solve the mixed field equations in a manner similar to that in Ref. [23, 24]. We diagonalize the mixing matrix  $M$  by an orthogonal transformation,  $OMO^T = M_D$ , where,

$$O = \begin{pmatrix} \cos \theta & -\sin \theta \\ \sin \theta & \cos \theta \end{pmatrix}, \quad (20)$$

where the angle  $\theta$  can be expressed as,

$$\tan 2\theta = \frac{2g_\phi\omega a^{-2}(a^2\mathcal{B})}{\left(\frac{\omega_p^2}{a} - m_\phi^2 a^2\right)}. \quad (21)$$

We assume that the mass of the pseudoscalar ( $m_\phi$ ) is negligible compared to the plasma frequency ( $\omega_p$ ).

### III. SIMULATIONS

We first generate the magnetic field numerically in wave vector space. This is relatively straightforward since it is uncorrelated for different wave vectors. The projection operator implies that the component of the magnetic field parallel to  $\mathbf{k}$  is zero. The two orthogonal components are uncorrelated. It is simplest to use polar coordinates  $(k, \theta, \phi)$  in wave vector space. Eq. 2 implies that for any wave vector  $\mathbf{k}$ ,  $b_k = 0$  and  $b_\theta$  and  $b_\phi$  are uncorrelated. We may, therefore, generate these by assuming the Gaussian distribution,

$$f(b_\theta(\mathbf{k}), b_\phi(\mathbf{k})) = N \exp \left[ - \left( \frac{b_\theta^2(\mathbf{k}) + b_\phi^2(\mathbf{k})}{2M(\mathbf{k})} \right) \right], \quad (22)$$

where  $N$  is the normalization factor. This represents an uncorrelated Gaussian distribution for the two components of the magnetic field in Fourier space, corresponding to the wave vector  $\mathbf{k}$ . Once we have these two components we can obtain the three Cartesian components of the magnetic field in wave vector space. Next we use Eq. 1 to obtain the three Cartesian components of the magnetic field in real space. The Gaussian random variates are generated by using the Numerical Recipes [90] code *gasdev*. The discrete Fourier transform is obtained by using the Recipes code *fourn*.

The optical polarizations are propagated, taking pseudoscalar-photon mixing into account by the procedure described in Ref. [79]. We need to propagate over a large number of magnetic domains from the quasar to the observer. We choose a fixed “external” coordinate system. The transverse component of the magnetic field in each domain is aligned at some angle to the fixed coordinate axes. In order to propagate through each domain we first rotate the coordinates so that the transverse magnetic field aligns along one of the coordinate axes. We then use standard expressions for pseudoscalar-photon mixing [79] in order to evaluate the correlation functions of the electromagnetic and pseudoscalar fields after propagation through the domain. We then rotate back to the fixed coordinate system. This procedure is repeated for propagation through each domain till the wave reaches the observer.

### IV. RESULTS

In this section we present the results of our numerical analysis. We first consider the case of flat space-time, ignoring cosmological evolution. Next we give results for the case of expanding universe. We set the following parameter values: plasma density  $n_e = 10^{-8} \text{ cm}^{-3}$ , frequency  $\nu = 10^6 \text{ GHz}$ , coupling  $g_\phi = 6.4 \times 10^{-11} \text{ GeV}^{-1}$  and mass  $m_\phi = 0$ . We shall use the spectral index  $n_B = -2.37$  but will also explore a range of values of this parameter. We perform most of our simulations on a grid size of  $1024 \times 1024 \times 1024$ , with the observer located at the center of the grid. The grid size is determined by the computing power available to us.

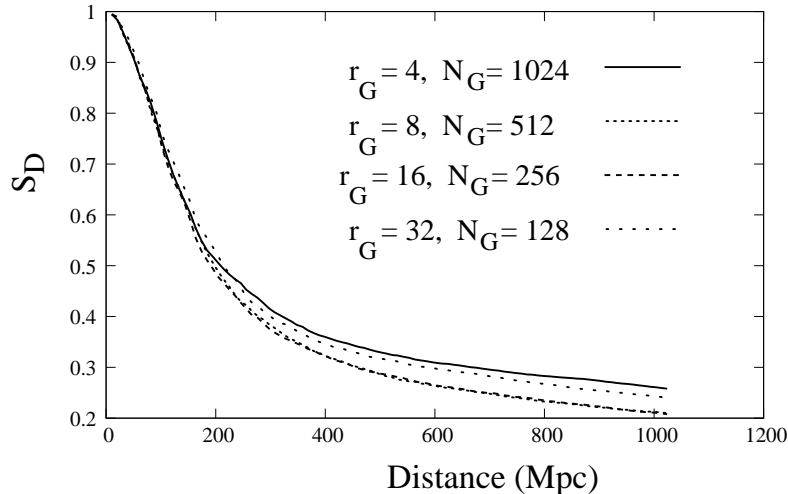


FIG. 1: The statistic  $S_D$  as a function of the distance between sources for different choices of the domain size  $r_G$  (in Mpc) and the number of points on the grid  $N_G$ . Here we have set  $n_B = -2.37$ .

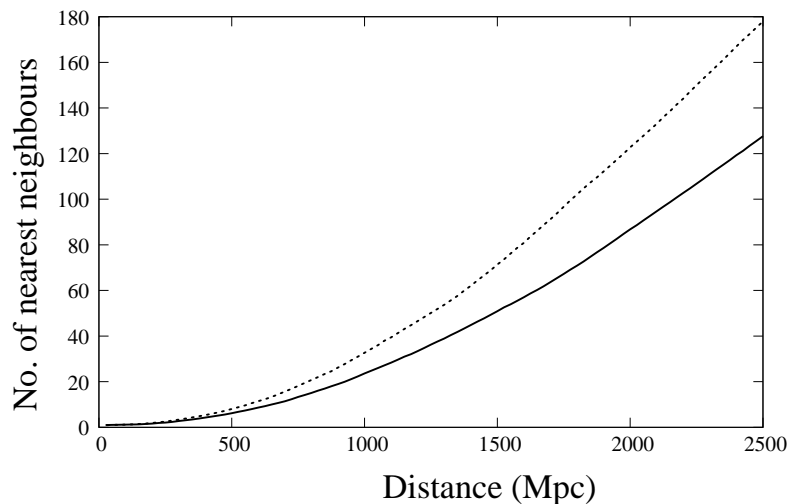


FIG. 2: The number of nearest neighbours as a function of distance. The upper curve (dashed) corresponds to angular diameter distance assuming a vacuum dominated universe. The lower curve (solid) is obtained assuming comoving distance in a matter dominated universe.

#### A. Flat space-time

Here we present our results ignoring cosmological evolution. We assume 200 quasars distributed randomly in space. The resulting statistic  $S_D$  as a function of the distance among sources is shown in Fig. 1. Results are presented for four different values of the domain size  $r_G = 4, 8, 16, 32$  Mpc. The number of points on the grid are suitably scaled so as to keep the total volume fixed. In Fig. 1 the statistic is computed by including all the sources that lie within a particular distance from a source. This fixes the number of nearest neighbours to be included for any distance. The real data has a total of 355 sources. The relationship between the number of nearest neighbours and the distance for the real data is shown in Fig. 2. We find that for a distance of 25 Mpc, the number of nearest neighbours is approximately 1. It becomes close to 2 only at a distance of about 200 Mpc. In Fig. 3 we show the fluctuations in

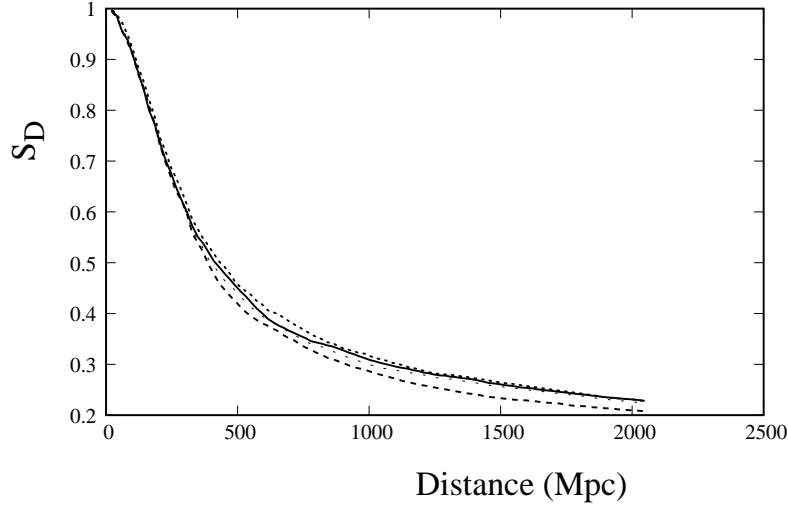


FIG. 3: The fluctuations in the statistic  $S_D$  for different choices of the random seed. Here we have set  $n_B = -2.37$ ,  $r_G = 8$  Mpc and the number of points on the grid  $N_G = 1024$ .

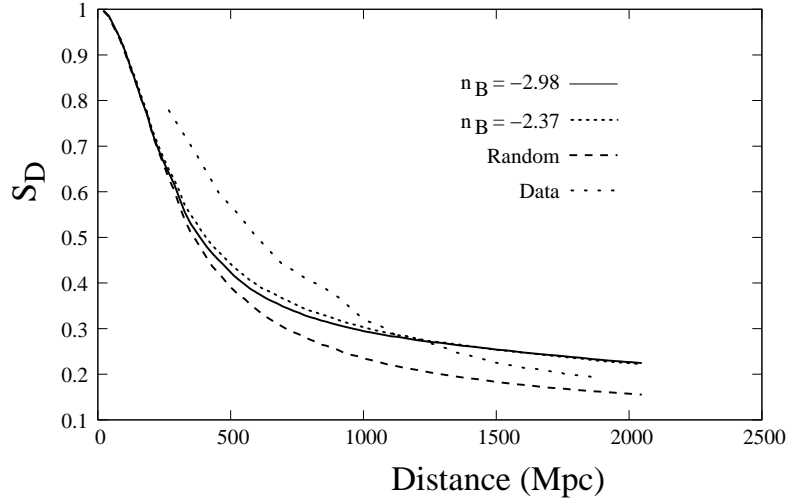


FIG. 4: Comparison of the simulation results with observed data. The dotted curve with large gaps shows the statistic obtained using observations. The remaining curves are obtained by simulations using parameters  $n_B = -2.37$  (dotted with small gaps),  $n_B = -2.98$  (solid), and a completely random magnetic field (dashed). Here we have set  $r_G = 8$  Mpc.

the statistic  $S_D$  for a given choice of parameters  $n_B = -2.37$ ,  $r_G = 8$  Mpc and the number of points on the grid,  $N_G = 1024$ . Results are shown for four different seeds used to initialize the simulations. We see significant fluctuations and hence to compare with data it is better to take the mean over several different computations. Finally in Fig. 4 we compare the simulation results with observations. The simulation results are shown for a mean of five different initializing seeds choosing  $n_B = -2.37$  and  $-2.98$ . Here we have set  $r_G = 8$  Mpc and the number of points on the grid equal to 1024. We also show results for the case where the background magnetic field is taken to be completely random. We find that the results for correlated magnetic fields show reasonable agreement with data. However, those with a random magnetic field are systematically below observations. We also find a relatively mild dependence on the exponent  $n_B$ . We conclude that pseudoscalar-photon mixing in a background magnetic field, described by Eqs. 1 and 2, gives reasonable agreement with observations. The small deviations from the data can be easily adjusted by



fine tuning the parameter values.

## B. Expanding Universe

In this section we present our results for the case of an expanding universe. We consider 355 sources, to exactly match the number of sources observed in the real data. The positions of these sources are also taken to be the same as in the data. The medium parameters, i.e. the magnetic field strength, the plasma density are taken to be the same as in the earlier non-expanding universe. Here these values are assumed to be their comoving values. The observed frequency  $\omega$  of the electromagnetic wave is assumed to be 2 eV. The comoving domain size is taken to be 15 Mpc. The Hubble constant is set equal to  $2.133h \times 10^{-42}$  GeV, with  $h = 0.7$ . Furthermore we assume matter dominated universe. As we shall see our results for the expanding universe are comparable to those obtained for flat space-time and hence such details do not make a very large difference to our final results.

We test our model against the data of the 355 sources observed by Hutsemékers et al. [2–4]. On placing the sources in our simulations at the same positions as in the data, we perform the propagation and calculate the Stokes parameters. We calculate the coordinate invariant statistics  $S_D$ , given in Eq. 6, for the observed polarizations and for the polarizations obtained from our simulations. The distribution of the linear polarization both for observed data and simulations is shown in Fig. 5. For the simulations we show results for  $n_B = -2.37$  and  $-2.95$ .

In Fig. 6, we show the statistic  $S_D$  for the data as well as the simulations. The simulation results are shown for a mean of five computations. We see that for both  $n_B = -2.37$  and  $-2.95$  the simulations show reasonable agreement with data. As mentioned above here we have set the domain size  $r_G = 15$  Mpc. It might be more reasonable to choose a smaller domain size. We find that as we reduce the domain size to  $r_G = 12$  Mpc, our statistic,  $S_D$ , becomes significantly larger than data. Hence we find even larger correlations in the optical polarizations. It may be possible to play with parameters to make our simulation results agree with observations in this case also. For example, this may be accomplished by decreasing the background magnetic field and/or the pseudoscalar-photon coupling constant  $g_\phi$ . However we postpone a detailed fit to future work since it requires extensive numerical simulations.

We may get some idea about the dependence of the statistic,  $S_D$ , on the domain size by performing simulations on a smaller grid. For this purpose we choose a grid size of  $256 \times 256 \times 256$ . We again take all the 355 sources but place them at a smaller radial distance with their polarizations and angular positions taken to be same as that of real data. The resulting statistic,  $S_D$ , as a function of the number of nearest neighbours is shown in Fig. 7 for four different domain sizes. The results are shown after averaging over 40 different simulations in order to reduce the effect of fluctuations. We find that  $S_D$  shows an oscillatory behaviour as a function of the domain size. It increases as we increase the domain size from 10 Mpc to 14 Mpc. However with a further increase from 14 Mpc to 16 Mpc it starts to decrease. Similar trend is seen for a larger grid of  $512 \times 512 \times 512$ . This suggests that for the range of parameters we consider,  $S_D$  shows an oscillatory dependence on the domain size. Furthermore the variation is significant but not very large. These results suggest that for the distance scale corresponding to the real data, the results may also show oscillations. Hence we expect to find a suitable fit to data even for smaller domain sizes with other parameters similar to what were chosen for the fit shown in Fig. 6.

## V. MIXING IN A MORE GENERAL BACKGROUND

As mentioned in the introduction a potential problem with our hypothesis is that the observed circular polarization in quasars is found to be negligible [4, 86]. However our model predicts a large circular polarization. We argued in the introduction that our model of the background medium, i.e. the magnetic field and the plasma density, may be unrealistic. The medium is expected to show fluctuations in time and space at any length scale relevant to propagation over cosmological distances. Here we have assumed that the magnetic field and the plasma density are time independent. Furthermore we have assumed that the magnetic field is uniform in a particular domain. In this section we determine how these assumptions affect our predictions for circular polarization.

### A. Space dependent magnetic field

We first examine how small scale spatial fluctuations in the magnetic field affect final results. We will continue to assume a uniform plasma density throughout this section. As discussed above, the magnetic field is likely to have fluctuations even on the scale of a single domain. Here we assume a simple model of space varying magnetic field,



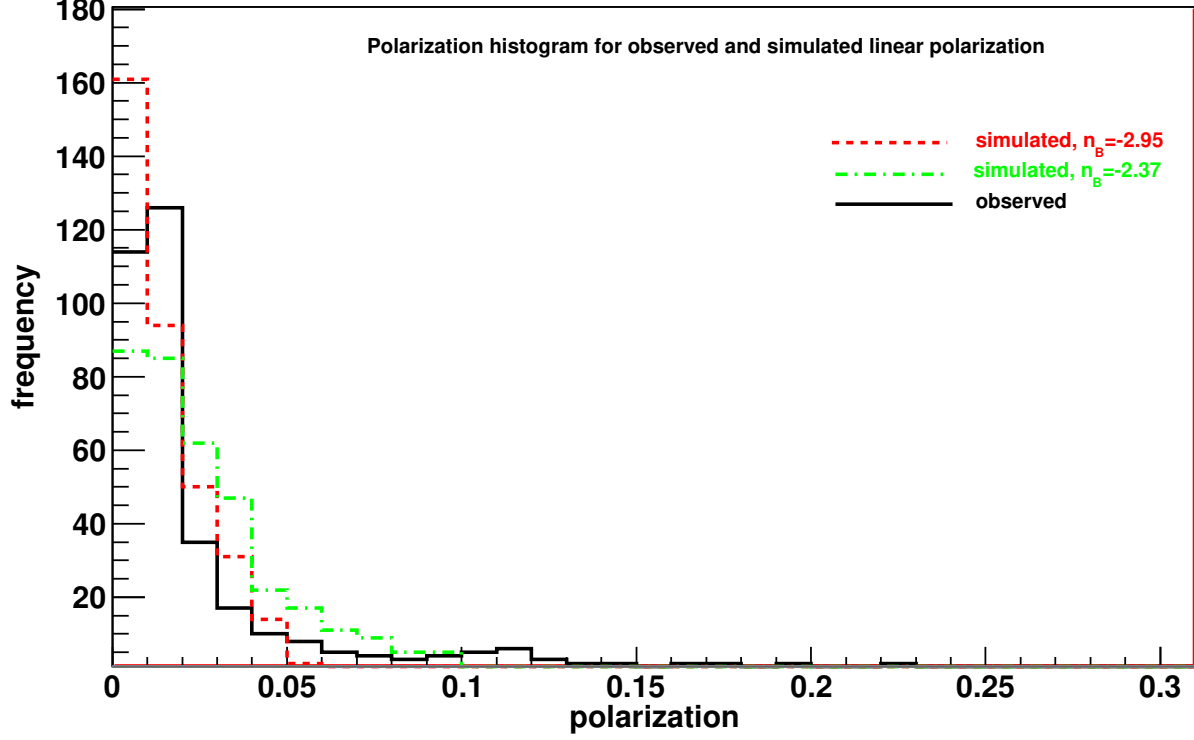


FIG. 5: The polarization histograms for the observed 355 sources (solid black curve) and for our simulations in an expanding universe. The red dashed curve and the green dash-dotted curve show results for  $n_B = -2.95$  and  $n_B = -2.37$  respectively.

given by,

$$\mathbf{B} = \mathcal{B}_0(\cos^2 \alpha \hat{\mathbf{x}} + \sin^2 \alpha \hat{\mathbf{y}}) \quad (23)$$

where,

$$\alpha = \frac{2\pi}{\lambda} \times z \quad (24)$$

and  $\lambda$  is the wavelength for the  $B$  field fluctuations. The rate at which the magnetic field changes with position  $z$  can be varied by changing the wavelength. Furthermore we point out that the field has been chosen such that its mean is not zero. The  $A$  and  $\chi$  field equations with this background can be written as,

$$(\omega + i\partial_z) \begin{pmatrix} \mathcal{A}_1 \\ \mathcal{A}_2 \\ \chi \end{pmatrix} - M \begin{pmatrix} \mathcal{A}_1 \\ \mathcal{A}_2 \\ \chi \end{pmatrix} = 0, \quad (25)$$

where,

$$M = \begin{pmatrix} \frac{\omega_p^2}{2\omega} & 0 & -\frac{g_\phi}{2}\mathcal{B}_0 \cos^2 \alpha \\ 0 & \frac{\omega_p^2}{2\omega} & -\frac{g_\phi}{2}\mathcal{B}_0 \sin^2 \alpha \\ -\frac{g_\phi}{2}\mathcal{B}_0 \cos^2 \alpha & -\frac{g_\phi}{2}\mathcal{B}_0 \sin^2 \alpha & \frac{m_\phi^2}{2\omega} \end{pmatrix}. \quad (26)$$

Here, we have approximated  $(\omega^2 + \partial_z^2) \approx 2\omega(\omega + i\partial_z)$  [20] and we have taken  $\mathbf{A}$  as  $(\mathcal{A}_1 \hat{\mathbf{x}} + \mathcal{A}_2 \hat{\mathbf{y}})$ . These equations are same as those given in Section [II B] with the scale factor  $a = 1$ .

Here we do not assume that the background magnetic field is changing sufficiently slowly so that we can choose basis vectors such that one of them points parallel to the transverse background magnetic field at any point  $z$  along

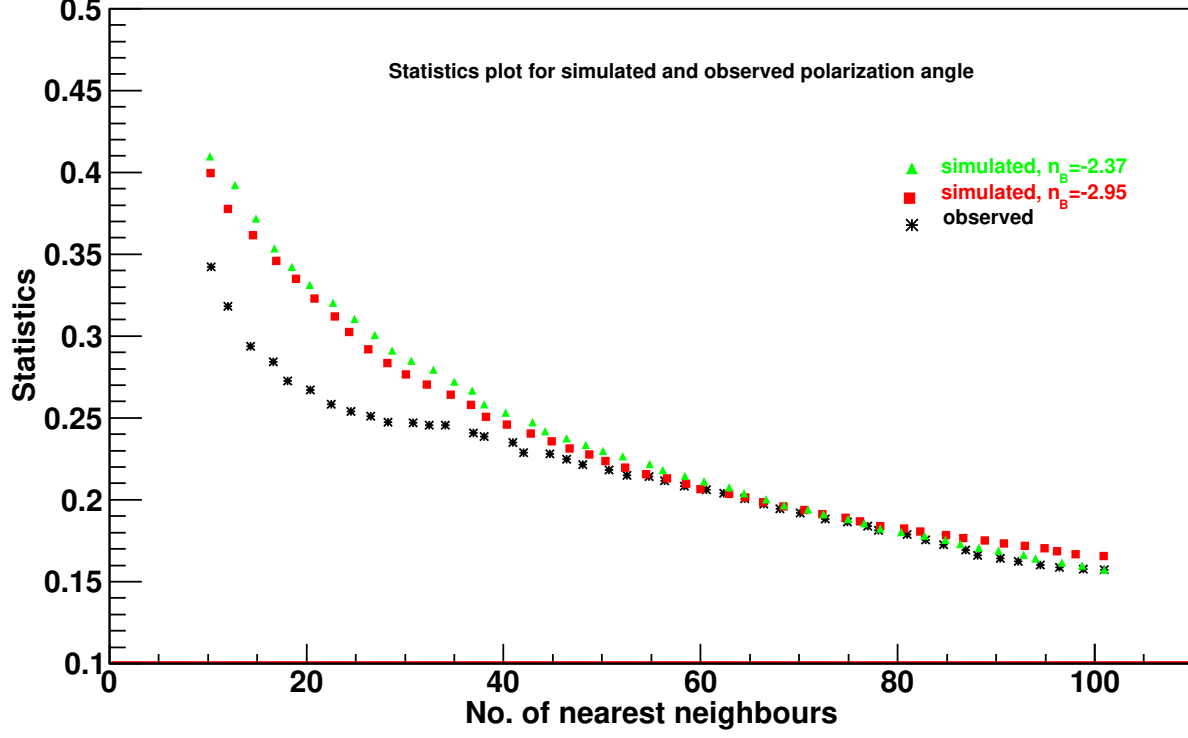


FIG. 6: The coordinate invariant statistic  $S_D$  as a function of the number of nearest neighbours for the 355 sources. The simulated results are shown by green triangles ( $n_B = -2.37$ ) and red squares ( $n_B = -2.95$ ), while the black crosses represent the observed data.

the path of the wave. This approximation would be valid if  $\lambda$  is very large but would break down for small  $\lambda$ . Instead we directly solve these equations numerically in terms of the density matrix which is defined as,

$$\rho(z) = \begin{pmatrix} \langle \mathcal{A}_1^*(z) \mathcal{A}_1(z) \rangle & \langle \mathcal{A}_1^*(z) \mathcal{A}_2(z) \rangle & \langle \mathcal{A}_1^*(z) \chi(z) \rangle \\ \langle \mathcal{A}_2^*(z) \mathcal{A}_1(z) \rangle & \langle \mathcal{A}_2^*(z) \mathcal{A}_2(z) \rangle & \langle \mathcal{A}_2^*(z) \chi(z) \rangle \\ \langle \chi^*(z) \mathcal{A}_1(z) \rangle & \langle \chi^*(z) \mathcal{A}_2(z) \rangle & \langle \chi^*(z) \chi(z) \rangle \end{pmatrix}. \quad (27)$$

The Stoke's parameters can be written as,

$$I(z) = \langle \mathcal{A}_1^*(z) \mathcal{A}_1(z) \rangle + \langle \mathcal{A}_2^*(z) \mathcal{A}_2(z) \rangle \quad (28)$$

$$Q(z) = \langle \mathcal{A}_1^*(z) \mathcal{A}_1(z) \rangle - \langle \mathcal{A}_2^*(z) \mathcal{A}_2(z) \rangle \quad (29)$$

$$U(z) = \langle \mathcal{A}_1^*(z) \mathcal{A}_2(z) \rangle + \langle \mathcal{A}_2^*(z) \mathcal{A}_1(z) \rangle \quad (30)$$

$$V(z) = i(\langle \mathcal{A}_1^*(z) \mathcal{A}_2(z) \rangle - \langle \mathcal{A}_2^*(z) \mathcal{A}_1(z) \rangle) \quad (31)$$

We assume that the wave is initially unpolarized and propagate in this medium over a distance of 10 Mpc. The resulting circular polarization  $|V|/I$  and the linear polarization  $\sqrt{Q^2 + U^2}/I$  is shown in Fig. 8 as a function of the wavelength  $\lambda$  of the background magnetic field. The figure clearly shows that for small  $\lambda$ , which corresponds to rapid fluctuations, the circular polarization is almost negligible as compared to the linear polarization. The value of linear polarization for small  $\lambda$  is comparable to that at large  $\lambda$ , where it starts to show large fluctuations. The circular polarization becomes comparable to linear polarization if the background varies slowly. Hence we clearly see that circular polarization is much smaller than linear polarization if the background magnetic field shows spatial fluctuations on sufficiently small length scales.

Here we have presented results only for a single domain. We do not attempt the more ambitious task of integrating over all the domains. That would be much more computationally intensive in comparison to the calculation performed in this paper since it would involve solving a system of differential equations in each domain. Furthermore it would

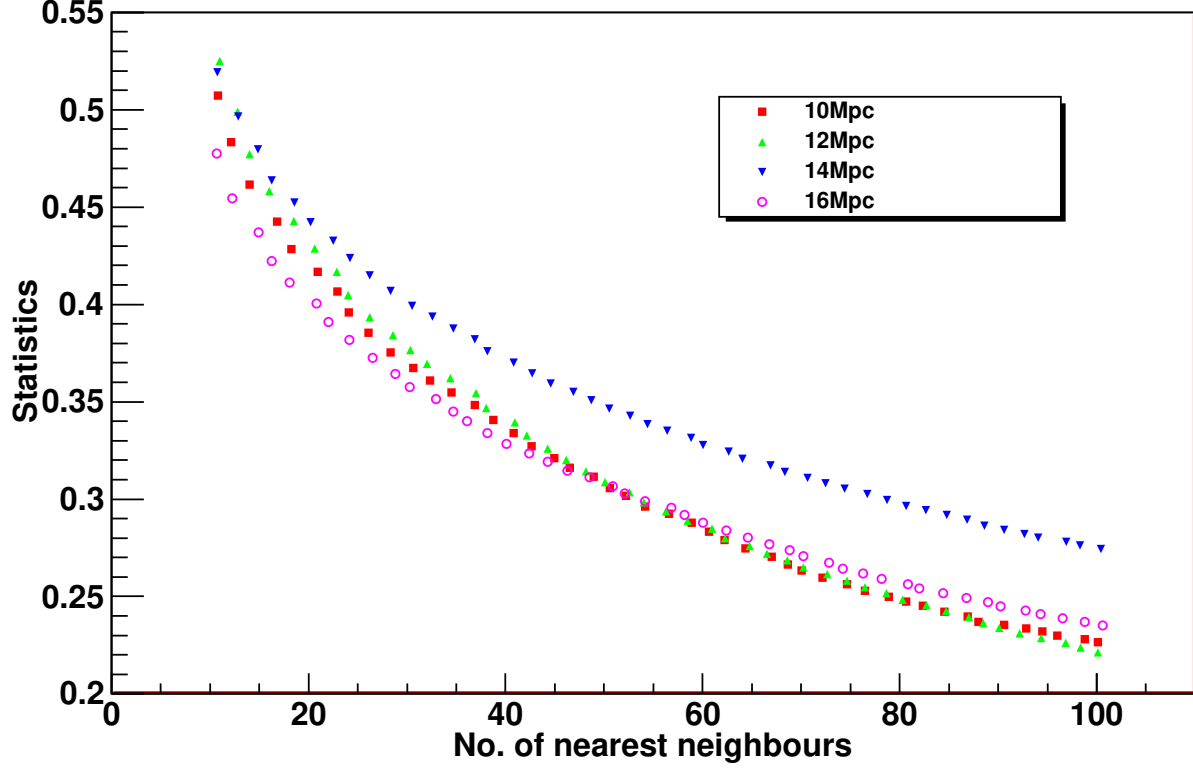


FIG. 7: The coordinate invariant statistic  $S_D$  as a function of the number of nearest neighbours for 355 sources. The sources are located at the same angular positions as real sources but their radial distance is reduced so that we can use a smaller grid of size  $256 \times 256 \times 256$ . Results are shown for four different domain sizes  $r_G = 10$  Mpc (red squares), 12 Mpc (green triangles), 14 Mpc (blue inverted triangles) and 16 Mpc (purple circles), after averaging over 40 different simulations. Here we have set  $n_B = -2.37$ .

depend on the precise model we use for the magnetic field in each domain. In any case our analysis in this section clearly shows that there exist very reasonable model of magnetic field which would lead to highly suppressed circular polarization.

### B. Time dependent background magnetic field

Another important issue that we consider is the possible time dependence of the background magnetic field. If the background magnetic field is time dependent, the pseudoscalar produced due to mixing with photons will not have the same frequency as that of the incident photon. Hence its correlation with photons may be significantly reduced. The circular polarization arises primarily due to reconversion of pseudoscalars back into photons. This generates a relative phase among the different components of the electromagnetic wave and hence leads to circular polarization. We see this explicitly by considering the evolution of the density matrix in a particular domain, given in Ref. [79],

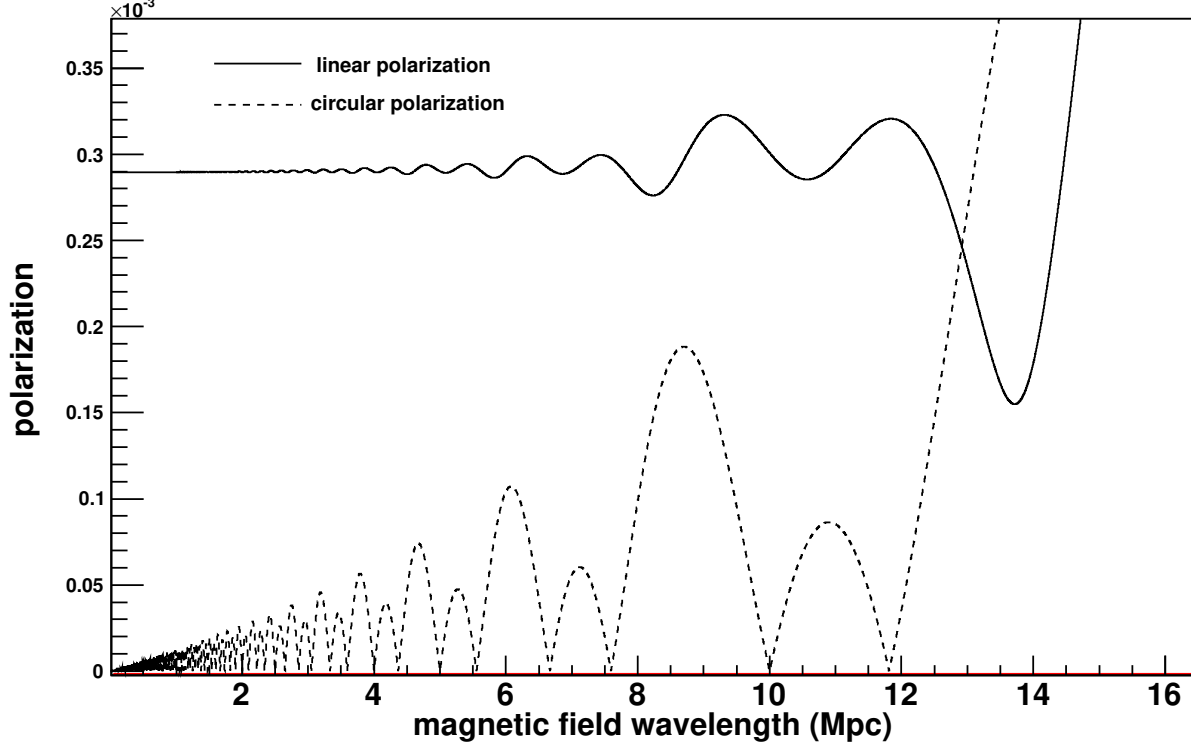


FIG. 8: The variation of linear (solid curve) and circular polarization (dashed curve) with respect to the wavelength  $\lambda$  of the background magnetic field.

reproduced here for convenience,

$$\begin{aligned}
 \langle A_{\parallel}(z)A_{\parallel}^*(z) \rangle &= \frac{1}{2} \langle A_{\parallel}(0)A_{\parallel}^*(0) \rangle \left[ 1 + \cos^2 2\theta + \sin^2 2\theta \cos[z(\Delta_{\phi} - \Delta_A)] \right] \\
 &+ \frac{1}{2} \langle \phi(0)\phi^*(0) \rangle \left[ \sin^2 2\theta - \sin^2 2\theta \cos[z(\Delta_{\phi} - \Delta_A)] \right] \\
 &+ \left\{ \frac{1}{2} \langle \phi(0)A_{\parallel}^*(0) \rangle \left[ \sin 2\theta \cos 2\theta - \sin 2\theta \cos 2\theta \cos[z(\Delta_{\phi} - \Delta_A)] \right] \right. \\
 &\quad \left. - i \sin 2\theta \sin[z(\Delta_{\phi} - \Delta_A)] \right\} + \text{c.c.} \quad (32)
 \end{aligned}$$

$$\langle A_{\perp}(z)A_{\perp}^*(z) \rangle = \langle A_{\perp}(0)A_{\perp}^*(0) \rangle \quad (33)$$

$$\begin{aligned}
 \langle A_{\perp}(z)A_{\parallel}^*(z) \rangle &= \langle A_{\perp}(0)A_{\parallel}^*(0) \rangle \left[ \cos^2 \theta e^{i F z} + \sin^2 \theta e^{i G z} \right] \\
 &+ \langle A_{\perp}(0)\phi^*(0) \rangle \left[ \sin \theta \cos \theta (e^{i F z} - e^{i G z}) \right] \quad (34)
 \end{aligned}$$

Here the vector  $\mathbf{A} = \mathbf{E}/\omega$ ,  $\omega$  is the frequency of the electromagnetic wave,  $\phi$  is the pseudoscalar field and  $A_{\parallel}$  and  $A_{\perp}$  respectively represent the components of  $\mathbf{A}$ , parallel and perpendicular to the transverse component of the background magnetic field. These equations give the density matrix elements after propagating through one domain, assuming a space and time independent magnetic field and plasma density. The circular polarization is governed by the correlation  $\langle A_{\perp}(z)A_{\parallel}^*(z) \rangle$ . Let us assume that initially this correlation is zero. Then after propagating through one domain, it becomes non-zero only if initially the correlation  $\langle A_{\perp}(0)\phi^*(0) \rangle$  is non-zero. We have assumed that at the source all the cross correlations are zero, i.e. the beam is unpolarized and the pseudoscalar field is zero. Hence circular polarization can be produced only if, after propagating through some domains, the correlation  $\langle A_{\perp}\phi^* \rangle$  becomes non-zero. However here we argue that if the background magnetic field is time-dependent, the frequency of

the pseudoscalar field produced due to mixing would be different from that of the electromagnetic field. Hence its correlation would be significantly reduced.

The pseudoscalar field equation may be written as,

$$\frac{\partial^2 \phi}{\partial t^2} - \nabla^2 \phi + m_\phi^2 \phi = g_\phi \mathbf{E} \cdot \mathbf{B} . \quad (35)$$

where  $\mathbf{B}$  represents the background magnetic field. Let us assume that the background magnetic field also undergoes fluctuations in time. Hence we may make a Fourier decomposition of this field. Here we assume that it contains only one significant component with frequency  $\Omega$ , i.e.  $|\mathbf{B}| \sim \cos(\Omega t)$ . The frequency of the electric field is  $\omega$ . It is clear from Eq. 35 that the frequency of the pseudoscalar produced has to be  $\omega' = \omega \pm \Omega$ .

Let us assume that the incident beam has a narrow spectral distribution, specified by the function  $A(\omega)$ , which denotes one of the components of the electromagnetic wave. We require correlations such as,  $\langle A(\omega')\phi^*(\omega') \rangle$ , where  $\omega' = \omega \pm \Omega$ . Since  $\phi(\omega') \propto A(\omega)e^{-i\omega't}$ , we have

$$\langle A(\omega')\phi^*(\omega') \rangle \propto \langle A(\omega')A^*(\omega) \rangle \quad (36)$$

It is clear that if  $\omega'$  is sufficiently different from  $\omega$ , this correlation would be vanishingly small. We expect this correlation to decrease rapidly with increase in the difference between the two frequencies. We point out that the background medium is expected to have fluctuations on all time scales. It is only after averaging out short time fluctuations that we expect it to show a somewhat smooth behaviour. Hence it may not be reasonable to assume that  $\Omega$  is close to zero. We point out that, although these temporal fluctuations may significantly affect the circular polarization, the mixing phenomenon would still generate significant linear polarization, as long as the mean value of the transverse component of the magnetic field is significantly different from zero. This is because the electromagnetic wave component parallel to the transverse magnetic field will decay into pseudoscalars and the perpendicular component will not. Hence we find that circular polarization may be significantly reduced compared to linear polarization if the background magnetic field shows sufficiently rapid fluctuations in time.

## VI. CONCLUSIONS

We have shown by direct simulations, both in a static and expanding universe, that the hypothesis of pseudoscalar-photon mixing is able to explain the observed alignment of optical polarizations from distant quasars for standard parameter values of the intergalactic magnetic field and plasma density. The value of pseudoscalar-photon coupling is taken to be close to its observational limit. The simulation results show reasonable agreement with data both with the distribution of linear polarization as well as the coordinate invariant statistic. Given the uncertainties in the medium parameters we have not performed the exercise of finding the best fit to the data. In any case before attempting a detailed fit it is necessary to perform further calculations to conclusively establish that pseudoscalar-photon mixing is indeed responsible for the alignment. One potential problem with this explanation, as discussed in the introduction, is the relatively large circular polarization predicted by this phenomenon [85]. However, there are many sources of decoherence which need to be properly taken into account before making a firm conclusion on the strength of circular polarization. We have explicitly shown that if the magnetic field shows fluctuations over the distance scale of individual domains, the circular polarization predicted by this phenomenon is significantly reduced in comparison to linear polarization. We find this phenomenon even for a relatively large wavelength of fluctuations, of order 1 Mpc, of the background magnetic field. Furthermore the agreement we find with data is potentially encouraging and hence this proposal may be taken seriously. It is possible that even if this precise mechanism is found not to explain the data consistently, a suitable generalization might work. We postpone such issues for future research.

## Acknowledgements

We thank Archana Kamal for useful discussions. We thank Subhayan Mandal for sharing with us his unpublished work on axion-photon mixing in an expanding universe.

- 
- [1] N. Agarwal, A. Kamal, and P. Jain, Phys. Rev. **D83**, 065014 (2011), 0911.0429.
  - [2] D. Hutsemékers, Astron. Astrophys. **332**, 410 (1998).

- [3] D. Hutsemékers and H. Lamy, *Astron. Astrophys.* **367**, 381 (2001), astro-ph/0012182.
- [4] D. Hutsemékers, R. Cabanac, H. Lamy, and D. Sluse, *Astron. Astrophys.* **441**, 915 (2005), astro-ph/0507274.
- [5] P. Jain, S. Panda, and S. Sarala, *Phys. Rev.* **D66**, 085007 (2002), hep-ph/0206046.
- [6] P. Jain, G. Narain, and S. Sarala, *Mon. Not. Roy. Astron. Soc.* **347**, 394 (2004), astro-ph/0301530.
- [7] A. Payez, J. R. Cudell, and D. Hutsemekers, *AIP Conf. Proc.* **1038**, 211 (2008), 0805.3946.
- [8] M. Y. Piotrovich, Y. N. Gnedin, and T. M. Natsvlshvili (2008), 0805.3649.
- [9] S. A. Joshi, R. A. Battye, W. A. Browne, N. Jackson, T. W. B. Muxlow, and P. N. Wilkinson, *Mon. Not. R. Astron. Soc.* **380**, 162 (2007).
- [10] K. Subramanian, T. R. Seshadri, and J. D. Barrow, *Mon. Not. Roy. Astron. Soc.* **344**, L31 (2003), astro-ph/0303014.
- [11] T. R. Seshadri and K. Subramanian, *Phys. Rev.* **D72**, 023004 (2005), astro-ph/0504007.
- [12] T. R. Seshadri and K. Subramanian, *Phys. Rev. Lett.* **103**, 081303 (2009), 0902.4066.
- [13] K. Jedamzik, V. Katalinic, and A. V. Olinto, *Phys. Rev.* **D57**, 3264 (1998), astro-ph/9606080.
- [14] K. Subramanian and J. D. Barrow, *Phys. Rev.* **D58**, 083502 (1998), astro-ph/9712083.
- [15] J. N. Clarke, G. Karl, and P. J. S. Watson, *Can. J. Phys.* **60**, 1561 (1982).
- [16] P. Sikivie, *Phys. Rev. Lett.* **51**, 1415 (1983).
- [17] P. Sikivie, *Phys. Rev.* **D32**, 2988 (1985).
- [18] P. Sikivie, *Phys. Rev. Lett.* **61**, 783 (1988).
- [19] L. Maiani, R. Petronzio, and E. Zavattini, *Phys. Lett.* **B175**, 359 (1986).
- [20] G. Raffelt and L. Stodolsky, *Phys. Rev.* **D37**, 1237 (1988).
- [21] E. D. Carlson and W. D. Garretson, *Phys. Lett.* **B336**, 431 (1994).
- [22] R. Bradley et al., *Rev. Mod. Phys.* **75**, 777 (2003).
- [23] S. Das, P. Jain, J. P. Ralston, and R. Saha, *JCAP* **0506**, 002 (2005), hep-ph/0408198.
- [24] S. Das, P. Jain, J. P. Ralston, and R. Saha, *Pramana* **70**, 439 (2008), hep-ph/0410006.
- [25] A. K. Ganguly, *Annals Phys.* **321**, 1457 (2006), hep-ph/0512323.
- [26] A. K. Ganguly, P. Jain, and S. Mandal, *Phys. Rev.* **D79**, 115014 (2009), 0810.4380.
- [27] R. D. Peccei and H. R. Quinn, *Phys. Rev. Lett.* **38**, 1440 (1977).
- [28] R. D. Peccei and H. R. Quinn, *Phys. Rev.* **D16**, 1791 (1977).
- [29] S. Weinberg, *Phys. Rev. Lett.* **40**, 223 (1978).
- [30] F. Wilczek, *Phys. Rev. Lett.* **40**, 279 (1978).
- [31] D. W. McKay, *Phys. Rev.* **D16**, 2861 (1977).
- [32] D. W. McKay and H. Munczek, *Phys. Rev.* **D19**, 985 (1979).
- [33] J. E. Kim, *Phys. Rev. Lett.* **43**, 103 (1979).
- [34] M. Dine, W. Fischler, and M. Srednicki, *Phys. Lett.* **B104**, 199 (1981).
- [35] J. E. Kim, *Phys. Rept.* **150**, 1 (1987).
- [36] D. Harari and P. Sikivie, *Phys. Lett.* **B289**, 67 (1992).
- [37] Z. G. Berezhiani, A. S. Sakharov, and M. Y. Khlopov, *Yadernaya Fizika* **55**, 1918 [*Sov. J. Nucl. Phys.* **55**, 1063] (1992).
- [38] S. Mohanty and S. N. Nayak, *Phys. Rev. Lett.* **70**, 4038 (1993), hep-ph/9303310.
- [39] P. Das, P. Jain, and S. Mukherji, *Int. J. Mod. Phys.* **A16**, 4011 (2001), hep-ph/0011279.
- [40] S. Kar, P. Majumdar, S. SenGupta, and A. Sinha, *Eur. Phys. J.* **C23**, 357 (2002), gr-qc/0006097.
- [41] S. Kar, P. Majumdar, S. SenGupta, and S. Sur, *Class. Quant. Grav.* **19**, 677 (2002), hep-th/0109135.
- [42] C. Csaki, N. Kaloper, and J. Terning, *Phys. Lett.* **B535**, 33 (2002), hep-ph/0112212.
- [43] C. Csaki, N. Kaloper, and J. Terning, *Phys. Rev. Lett.* **88**, 161302 (2002), hep-ph/0111311.
- [44] Y. Grossman, S. Roy, and J. Zupan, *Phys. Lett.* **B543**, 23 (2002), hep-ph/0204216.
- [45] Y.-S. Song and W. Hu, *Phys. Rev.* **D73**, 023003 (2006), astro-ph/0508002.
- [46] A. Mirizzi, G. G. Raffelt, and P. D. Serpico, *Phys. Rev.* **D72**, 023501 (2005), astro-ph/0506078.
- [47] G. G. Raffelt, *Lect. Notes Phys.* **741**, 51 (2008), hep-ph/0611350.
- [48] Y. N. Gnedin, M. Y. Piotrovich, and T. M. Natsvlshvili, *Mon. Not. Roy. Astron. Soc.* **374**, 276 (2007), astro-ph/0607294.
- [49] A. Mirizzi, G. G. Raffelt, and P. D. Serpico, *Phys. Rev.* **D76**, 023001 (2007), 0704.3044.
- [50] F. Finelli and M. Galaverni, *Phys. Rev.* **D79**, 063002 (2009), 0802.4210.
- [51] A. De Angelis, O. Mansutti, M. Persic, and M. Roncadelli, *Mon. Not. Roy. Astron. Soc.* **394**, L21 (2009).
- [52] A. De Angelis, G. Galanti, and M. Roncadelli, *Phys. Rev.* **D84**, 105030 (2011).
- [53] A. De Angelis, M. Roncadelli, and O. Mansutti, *Phys. Rev.* **D76**, 121301 (2007).
- [54] L. Ostman and E. Mortsell, *JCAP* **0502**, 005 (2005), astro-ph/0410501.
- [55] D. Lai and J. Heyl, *Phys. Rev.* **D74**, 123003 (2006), astro-ph/0609775.
- [56] D. Hooper and P. D. Serpico, *Phys. Rev. Lett.* **99**, 231102 (2007), 0706.3203.
- [57] K. A. Hochmuth and G. Sigl, *Phys. Rev.* **D76**, 123011 (2007), 0708.1144.
- [58] D. Chelouche, R. Rabadan, S. Pavlov, and F. Castejon, *Astrophys. J. Suppl.* **180**, 1 (2009), 0806.0411.
- [59] D. A. Dicus, E. W. Kolb, V. L. Teplitz, and R. V. Wagoner, *Phys. Rev.* **D18**, 1829 (1978).
- [60] M. I. Vysotskii, Y. B. Zel'Dovich, M. Y. Khlopov, and V. M. Chechetkin, *JETP Lett.* **27**, 502 (1978).
- [61] D. S. P. Dearborn, D. N. Schramm, and G. Steigman, *Phys. Rev. Lett.* **56**, 26 (1986).
- [62] G. G. Raffelt and D. S. P. Dearborn, *Phys. Rev.* **D36**, 2211 (1987).
- [63] G. Raffelt and D. Seckel, *Phys. Rev. Lett.* **60**, 1793 (1988).
- [64] M. S. Turner, *Phys. Rev. Lett.* **60**, 1797 (1988).
- [65] H.-T. Janka, W. Keil, G. Raffelt, and D. Seckel, *Phys. Rev. Lett.* **76**, 2621 (1996), astro-ph/9507023.

- [66] W. Keil et al., Phys. Rev. **D56**, 2419 (1997), astro-ph/9612222.
- [67] J. W. Brockway, E. D. Carlson, and G. G. Raffelt, Phys. Lett. **B383**, 439 (1996), astro-ph/9605197.
- [68] J. A. Grifols, E. Masso, and R. Toldra, Phys. Rev. Lett. **77**, 2372 (1996), astro-ph/9606028.
- [69] G. G. Raffelt, Ann. Rev. Nucl. Part. Sci. **49**, 163 (1999), hep-ph/9903472.
- [70] L. J. Rosenberg and K. A. van Bibber, Phys. Rept. **325**, 1 (2000).
- [71] K. Zioutas et al. (CAST), Phys. Rev. Lett. **94**, 121301 (2005), hep-ex/0411033.
- [72] W. M. Yao et al. (Particle Data Group), J. Phys. **G33**, 1 (2006).
- [73] J. Jaeckel, E. Masso, J. Redondo, A. Ringwald, and F. Takahashi, Phys. Rev. **D75**, 013004 (2007), hep-ph/0610203.
- [74] S. Andriamonje et al. (CAST), JCAP **0704**, 010 (2007), hep-ex/0702006.
- [75] C. Robilliard et al., Phys. Rev. Lett. **99**, 190403 (2007), 0707.1296.
- [76] E. Zavattini et al. (PVLAS), Phys. Rev. **D77**, 032006 (2008), 0706.3419.
- [77] A. Rubbia and A. S. Sakharov, Astropart. Phys. **29**, 20 (2008), 0708.2646.
- [78] S. Lee, G.-C. Liu, and K.-W. Ng, Phys. Rev. **D73**, 083516 (2006), astro-ph/0601333.
- [79] N. Agarwal, P. Jain, D. W. McKay, and J. P. Ralston, Phys. Rev. **D78**, 085028 (2008), 0807.4587.
- [80] N. Bassan, A. Mirizzi, and M. Roncadelli, JCAP **05**, 010 (2010).
- [81] D. G. Yamazaki, K. Ichiki, T. Kajino, and G. J. Mathews, Phys. Rev. **D81**, 023008 (2010), 1001.2012.
- [82] A. De Angelis, M. Persic, and M. Roncadelli, Mod. Phys. Lett. **A23**, 315 (2008).
- [83] J. W. Armstrong, B. J. Rickett, and S. R. Spangler, The Astrophysical Journal **443**, 209 (1995).
- [84] A. H. Minter and S. R. Spangler, The Astrophysical Journal **458**, 194 (1996).
- [85] A. Payez, J. R. Cudell, and D. Hutsemékers (2011), 1107.2013.
- [86] D. Hutsemékers, B. Borguet, D. Sluse, R. Cabanac, and H. Lamy, Astron. Astrophys. **520**, L7 (2010), 1009.4049.
- [87] S. A. Carroll and G. B. Field, Phys. Rev. **D43**, 3789 (1991).
- [88] D. W. Garretson, G. B. Field, and S. A. Carroll, Phys. Rev. **D46**, 5346 (1992).
- [89] J.-R. Cudell and S. Mandal, unpublished (2011).
- [90] W. H. Press, S. A. Teukolsky, W. T. Vetterling, and B. P. Flannery, *Numerical Recipes in Fortran, second edition* (Cambridge University Press, 1992).